

Diversity of orientational transitions in the $\text{Dy}_x\text{Er}_{1-x}\text{CrO}_3$ system

A. M. Kadomtseva, M. D. Kuz'min, M. M. Lukina, and A. A. Mukhin

M. V. Lomonosov State University, Moscow

(Submitted 16 February 1988)

Zh. Eksp. Teor. Fiz. **94**, 251–258 (September 1988)

Spontaneous orientational transitions between the main magnetic configurations $\Gamma_2(G_zF_x) \rightarrow \Gamma_4(G_xF_z) \rightarrow \Gamma_1(G_y)$ were discovered during cooling of orthochromites of the system $\text{Dy}_x\text{Er}_{1-x}\text{CrO}_3$ ($x = 0.2$ and 0.3). A study was made of various orientational transitions in a magnetic field \mathbf{H} applied along the \mathbf{a} and \mathbf{c} axes. The corresponding H - T phase diagrams were constructed. The H_x - T phase diagram had a bicritical point of convergence of two lines representing second-order phase transitions $\Gamma_{12} \rightleftharpoons \Gamma_2$ and $\Gamma_{24} \rightleftharpoons \Gamma_2$, and a line representing a first-order phase transition between canted phases $\Gamma_{24} \rightleftharpoons \Gamma_{12}$. An allowance for the nature of the anisotropy of the exchange splitting of the ground doublet of the Dy^{3+} and Er^{3+} ions was made in an analysis of the mechanisms of the observed phase transitions, and the calculated H_x - T and H_z - T phase diagrams were in agreement with the experiments.

INTRODUCTION

Magnetic properties of dysprosium and erbium orthochromites are very different. At all temperatures below $T_N = 142$ K dysprosium orthochromite has a stable magnetic structure $\Gamma_2(G_zF_x)$ (Refs. 1 and 2). In the case of erbium orthochromite below $T_N = 133$ K there is a magnetic structure $\Gamma_4(G_xF_z)$, but cooling to $T_M = 9.3$ K results in a spin-reorientation transition to an antiferromagnetic state $\Gamma_1(G_y)$, known as the Morin transition.^{3,4} Such a difference in the behavior of these orthochromites is due to the anisotropy of the R-Cr exchange interaction, particularly the anisotropy of splitting of the ground-state doublet of the Er^{3+} and Dy^{3+} ions because of the R-Cr exchange. This stabilizes different magnetic structures in these compounds. It would be of interest to vary the concentrations of the Dy^{3+} and Er^{3+} ions in orthochromites and obtain a composition in which the competition between the Dy-Cr and Er-Cr anisotropic exchange processes would induce different types of spontaneous and field-induced spin-reorientation transitions providing an opportunity to check and understand better the nature of the mechanisms responsible for the magnetic anisotropy of orthochromites.

EXPERIMENTAL RESULTS

We investigated $\text{Dy}_x\text{Er}_{1-x}\text{CrO}_3$ ($x = 0.2, 0.3$) single crystals grown from a molten solution by isothermal evaporation and we measured the magnetization (using a vibrating magnetometer) and the magnetostriction (using strain gauges) at temperatures 1.5–150 K in the field of a superconducting solenoid ranging up to 60 kOe. Measurements of the magnetization curves along different crystallographic axes established that in the case of the investigated crystals there were two types of spin-reorientational transitions: $\Gamma_2 \rightleftharpoons \Gamma_4$ and $\Gamma_4 \rightleftharpoons \Gamma_1$.

Figure 1 shows the temperature dependence of the spontaneous magnetization m for the composition with $x = 0.3$ found by extrapolation of the magnetization isotherms to zero field. We can see that below $T_N = 127$ K the weak ferromagnetic moment was oriented along the \mathbf{a} axis of an orthorhombic crystal with the $\Gamma_2(G_zF_x)$ magnetic structure. Cooling resulted in reorientation at $T_R = 14$ K from the \mathbf{a} to the \mathbf{c} axis (orientational transition $\Gamma_2 \rightleftharpoons \Gamma_4$) and

further cooling to $T_M = 5.9$ K destroyed the weak ferromagnetism so that the crystal became antiferromagnetic (Morin-type transition $\Gamma_4 \rightleftharpoons \Gamma_1$); the latter orientational transition $\Gamma_4 \rightleftharpoons \Gamma_1$ was abrupt representing a first-order phase transition. Similar transitions at $T_R = 17$ K and $T_M = 7.8$ K were observed also for the composition with $x = 0.2$. Therefore, cooling of the $\text{Dy}_x\text{Er}_{1-x}\text{CrO}_3$ system ($x = 0.2, 0.3$) revealed all three types of the magnetic structure, Γ_1 , Γ_2 , and Γ_4 , compatible with the crystal symmetry.

The application of an external magnetic field $\mathbf{H} \parallel \mathbf{c}$ induced at temperatures $T < T_M$ an orientational transition $\Gamma_1 \rightleftharpoons \Gamma_4$, as demonstrated clearly by the magnetization curves and those representing the magnetostriction λ , which were typically of the kind shown in Fig. 2. Clearly, in low fields the magnetization (curve 1) and the magnetostriction were practically equal to zero and only after passing through a threshold field $H^h \approx 0.7$ kOe did we find that the $m(H)$ and $\lambda(H)$ curves exhibited inflections followed by a rapid rise of the magnetization and magnetostriction, which was completed in fields of the order of several kilo-oersted. An allowance for a demagnetizing field had the effect that the $\Gamma_1 \rightleftharpoons \Gamma_4$ transition occurred abruptly in a field corresponding to a lower inflection of the magnetization and magnetostriction curves.

The extended nature of the transition, demonstrated in Figs. 2a and 2b, was clearly associated with the presence of an intermediate state which appeared as a result of a first-order phase transition. The width of the transition on the field scale was less for a sample used to investigate the magnetization. This sample was a plate of $3.6 \times 2.7 \times 0.8$ mm dimensions with the long side parallel to the field (demagnetization factor $N_z \approx 2$). The magnetostriction was investigated employing a more complex sample ($N_z \approx 4.6$); the range of existence of the intermediate state was wider. We determined the temperature dependences of the fields corresponding to the onset and completion of a reorientational transition (H_z - T phase diagram) for a sample with $N_z = 4.6$ (Fig. 3) and identified the region of the intermediate state. Clearly, the field corresponding to the onset of the phase transition vanished at the point T_M , whereas the field corresponding to the completion of the transition remained finite and similar in value to the demagnetizing field. We also in-

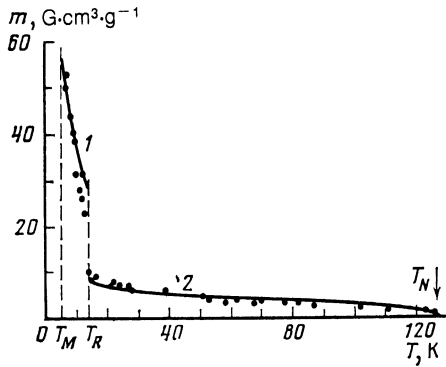


FIG. 1. Temperature dependences of the spontaneous magnetization along the **a** and **c** axes obtained for a $\text{Dy}_{0.3}\text{Er}_{0.7}\text{CrO}_3$ single crystal: 1) m_z ; 2) m_c . The continuous curve calculated in the one-doublet approximation and the points are the experimental values.

cluded in Fig. 3 (on the right) the H_z - T phase diagram for a spin-reorientational transition $\Gamma_{24} \rightleftharpoons \Gamma_4$ induced by a field $\mathbf{H} \parallel \mathbf{c}$ at temperatures $T > T_R = 14$ K. The threshold field for this transition was deduced from an inflection of the magnetization curves corresponding to completion of the process of spin reorientation (curve 3 in Fig. 2a). A similar phase diagram was also obtained for the sample with $\kappa = 0.2$.

The greatest diversity of the orientational transitions was exhibited by $\text{Dy}_\kappa\text{Er}_{1-\kappa}\text{CrO}_3$ in fields $\mathbf{H} \parallel \mathbf{a}$. The field dependence of the magnetostriction was then more complex (Fig. 4). At temperatures $T < T_M = 5.9$ K the composition with $\kappa = 0.3$ exhibited in fields $\mathbf{H} \parallel \mathbf{a}$ a positive magnetostriction corresponding to smooth rotation of the spins in the bc plane as a result of an orientational transition $\Gamma_{12} \rightleftharpoons \Gamma_2$, completed when the field reached $H^{\text{th}} \approx 20$ – 30 kOe. The magnetostriction isotherms were most complex in the temperature range $T_M = 5.9$ K $< T < T_Q = 6.4$ K (T_Q is the temperature corresponding to the bicritical point) where in the range of low fields of the order of several kilo-oersted there was an abrupt change of the magnetostriction to the negative range followed by an increase with the field up to $H^{\text{th}} \approx 20$ kOe,

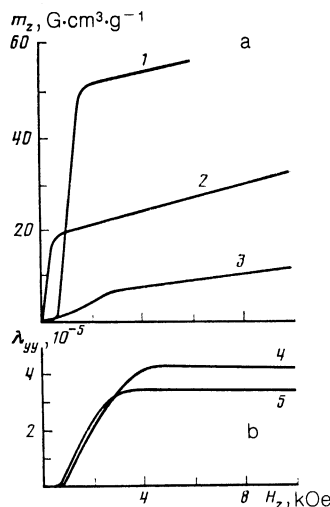


FIG. 2. Isotherms of the magnetization (a) and the magnetostriction (b) in $\mathbf{H} \parallel \mathbf{c}$: 1), 5) $T = 4.2$ K; 2) 10.6 K; 3) 25.6 K; 4) $T = 1.5$ K.

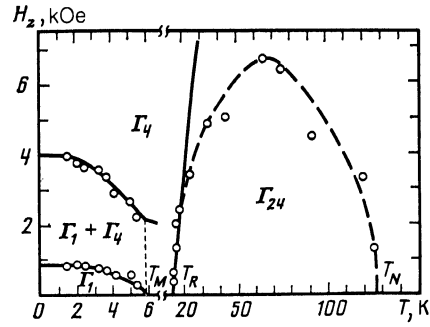


FIG. 3. Phase (H_z - T) diagram for the composition with $\kappa = 0.3$. The continuous curves are calculated; the circles and the dashed line are the experimental results; the dotted line represents the position of T_M .

when the spin reorientation was completed. We shall show below that the negative jump of the magnetostriction was due to rotation of the spins in a field $\mathbf{H} \parallel \mathbf{a}$ from the ac plane to the bc plane ($\Gamma_{12} \rightleftharpoons \Gamma_{24}$), and the subsequent rise was due to further reorientation of the spins toward the **c** axis creating the Γ_2 ($G_z F_x$) magnetic structure. At temperatures above 6.4 K the magnetostriction was negative and corresponded to the $\Gamma_{24} \rightleftharpoons \Gamma_2$ orientational transition. The H_x - T phase diagram is shown in Fig. 5. The magnetostriction curves and the phase diagram for the composition with $\kappa = 0.2$ obtained in fields $\mathbf{H} \parallel \mathbf{a}$ were qualitatively the same as those shown in Figs. 4 and 5 for the composition with $\kappa = 0.3$.

THEORY AND DISCUSSION OF RESULTS

In describing the phase transitions observed in the $\text{Dy}_\kappa\text{Er}_{1-\kappa}\text{CrO}_3$ system at low temperatures ($T < 50$ K) it is sufficient to consider only the ground-state doublets of the Er^{3+} and Dy^{3+} ions separated from excited states by intervals ≈ 50 K for ErCrO_3 (Ref. 5) and ≈ 75 K according to the data for Dy^{3+} in DyFeO_3 (Ref. 6). We shall represent the energy levels of the ground-state doublet in the form^{7,8}

$$E_{Ri}^{(1,2)} = \Delta E_{Ri}^{\text{VV}}(\mathbf{H}, \mathbf{G}) \pm \Delta R^i(\mathbf{H}, \mathbf{G}), \quad (1)$$

where $i = \pm$ distinguishes two inequivalent positions of the rare-earth ions and $\Delta E_{Ri}^{\text{VV}}$ is the shift (of the Van Vleck type) of the center of gravity of the ground-state doublet due to mixing of excited states as a result of the R-Cr exchange

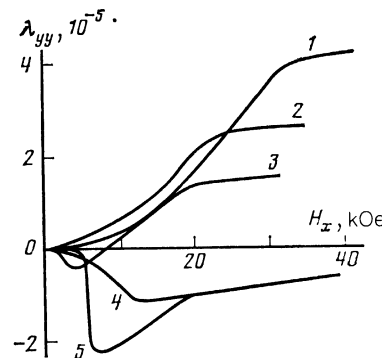


FIG. 4. Isotherm of the magnetostriction of $\text{Dy}_{0.3}\text{Er}_{0.7}\text{CrO}_3$ in $\mathbf{H} \parallel \mathbf{a}$: 1) $T = 1.5$ K; 2) 5.4 K; 3) 5.9 K; 4) 7.1 K; 5) 6.1 K.

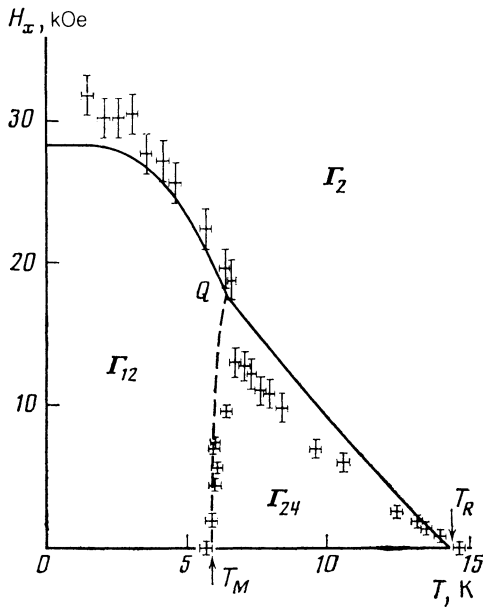


FIG. 5. Phase (H_x - T) diagram of $\text{Dy}_{0.3}\text{Er}_{0.7}\text{CrO}_3$. The points are the experimental values, whereas the continuous and dashed curves are calculated (the continuous curves correspond to a second-order phase transition and the dashed line corresponds to a first-order transition); Q is the bicritical point.

interaction and the interaction with an external field. Without specifying the explicit form of $\Delta E_{Ri}^{\text{VV}}$, we shall allow for it by renormalization of the thermodynamic potential of Cr subsystem. The quantities Δ_R^i governing the half-splitting of the ground-state doublets of the Dy^{3+} and Er^{3+} ions are

$$\Delta_{\text{Dy}}^{\pm} = \mu_x^0 H_x + \Delta_z^0 G_z \pm \mu_y^0 H_y, \quad (2)$$

$$(\Delta_{\text{Er}}^{\pm})^2 = (\mu_{xx} H_x + \Delta_z' G_z \pm \mu_{xy} H_y)^2 + (\mu_{yy} H_y \pm \Delta_z'' G_z \pm \mu_{yx} H_x)^2 + (\mu_{zz} H_z + \Delta_x G_x \pm \Delta_y G_y)^2, \quad (3)$$

where $\Delta_x, \Delta_y, \Delta_z = [(\Delta_x')^2 + (\Delta_x'')^2]^{1/2}$, and Δ_z^0 represent the half-splitting of the doublets due to the R-Cr interaction in the $\Gamma_4(G_x), \Gamma_1(G_y),$ and $\Gamma_2(G_z)$ phases; the effective magnetic moments are $\mu_{\alpha\beta} = \mu_B g_{\alpha\beta}/2$, where $g_{\alpha\beta}$ is the g tensor of the doublet. The difference between Δ_{Dy}^{\pm} and Δ_{Er}^{\pm} is due to the fact that the Dy^{3+} ion is of the Ising type,² i.e., it becomes magnetized only parallel or antiparallel to a specific axis lying in the ab plane and oriented at an angle $\alpha_{\pm} = \pm \tan^{-1}(\mu_y^0/\mu_x^0)$ relative to the a axis. For simplicity, Eq. (3) is derived ignoring the R-R interaction, which is not of fundamental importance in the effects under consideration.

According to Ref. 2, in the case of DyCrO_3 , we have

$$\Delta_z^0 = 0.84 \text{ K}, \quad \mu_x^0 = 4.13 \mu_B, \quad (4a)$$

whereas the results of Ref. 3 give for ErCrO_3

$$\begin{aligned} \Delta_x &= 4.45 \text{ K}, \quad \Delta_y = 4.8 \text{ K}, \quad \Delta_z = 3.2 \text{ K}, \quad \mu_{zz} = 5.65 \mu_B, \\ \mu_x &= (\mu_{xx}^2 + \mu_{yx}^2)^{1/2} = 2.95 \mu_B, \quad \bar{\mu}_x = (\mu_{xx} \Delta_z' + \mu_{yx} \Delta_z'') / \Delta_z = 1.0 \mu_B. \end{aligned} \quad (4b)$$

The thermodynamic potential of the system per one formula unit can be represented in the form^{7,8}

$$\Phi = \bar{\Phi}_{\text{Cr}} - \frac{T}{2} \sum_{i=\pm} \left[\kappa \ln \left(2 \text{ch} \frac{\Delta_{\text{Dy}}^i}{T} \right) + (1-\kappa) \ln \left(2 \text{ch} \frac{\Delta_{\text{Er}}^i}{T} \right) \right], \quad (5)$$

where

$$\begin{aligned} \bar{\Phi}_{\text{Cr}} &= \Phi_{\text{Cr}} + \frac{1}{2} \sum_i \left[\kappa \Delta E_{\text{Dy}_i}^{\text{B}\Phi} + (1-\kappa) \Delta E_{\text{Er}_i}^{\text{B}\Phi} \right] = \frac{1}{2} K_{ac}^0 G_z^2 \\ &+ \frac{1}{2} K_{ab}^0 G_y^2 - m_x^0 H_x G_z - m_z^0 H_z G_x - \frac{1}{2} \chi_{\perp} [H^2 - (\mathbf{HG})^2] \end{aligned} \quad (6)$$

is the thermodynamic potential of the Cr subsystem renormalized by the Van Vleck corrections: $K_{ac,ab}^0 = K_{ac,ab}^{\text{Cr}} + \kappa K_{ac,ab}^{\text{Dy}} + (1-\kappa) K_{ac,ab}^{\text{Er}}$, where $m_{x,z}^0$ are the weak ferromagnetic moments, and χ_{\perp} is the transverse susceptibility of the Cr subsystem. The majority of the observed properties of the $\text{Dy}_{z'}\text{Er}_{1-z'}\text{CrO}_3$ system can be described simply by adopting the high-temperature approximation ($\Delta_R \ll T$) for Φ , where

$$\begin{aligned} \Phi &= \Phi_0 - \frac{1}{2} \chi_{\perp} [H^2 - (\mathbf{HG})^2] - m_x H_x G_z - m_z H_z G_x \\ &+ \frac{1}{2} K_{ac} G_z^2 + \frac{1}{2} K_{ab} G_y^2 + \frac{1}{2} K_{ab}' G_x^2 G_y^2 + \Delta \Phi(\mathbf{G}), \end{aligned} \quad (7)$$

where the term Φ_0 is independent of \mathbf{G} ,

$$\begin{aligned} m_z &= m_z^0 + (1-\kappa) \mu_{zz} \Delta_z / T, \\ m_x &= m_x^0 + \kappa \mu_x^0 \Delta_z^0 / T + (1-\kappa) \bar{\mu}_x \Delta_z / T, \\ K_{ac} &= K_{ac}^0 - \kappa (\Delta_x^0)^2 / T + (1-\kappa) (\Delta_x^2 - \Delta_z^2) / T, \\ K_{ab} &= K_{ab}^0 + (1-\kappa) (\Delta_x^2 - \Delta_y^2) / T, \quad K_{ab}' = 2 \Delta_x^2 \Delta_y^2 / 3 T^3, \\ \Delta \Phi(\mathbf{G}) &= \{ \kappa (\Delta_x^0)^4 G_z^4 + (1-\kappa) [(\Delta_x^2 - \Delta_y^2) G_z^2 \\ &- (\Delta_y^2 - \Delta_x^2) G_y^2]^2 \} / 12 T^3. \end{aligned} \quad (8)$$

In the subsequent analysis, allowing for the smallness of Δ_z^0 in the case of Dy^{3+} ($\approx 0.84 \text{ K}$) and for the relatively weak anisotropy of the exchange splitting in the case of Er^{3+} ($|\Delta_{y,z}^2 - \Delta_x^2| \ll \Delta_x^2$) [see Eq. (4)], we shall ignore the term $\Delta \Phi(\mathbf{G})$ in Eq. (7), but retain the term $K_{ab}' G_x^2 G_y^2$ which is sufficiently large and determines the nature of the process of spin reorientation in the ab plane.

We shall first analyze the spontaneous orientational transitions ($H = 0$). The $\Gamma_2(G_z) \rightleftharpoons \Gamma_4(G_x)$ reorientation at $T_R = 14 \text{ K}$ occurs when the sign of K_{ac} is reversed see Eq. (7) as a result of competition between the exchange splitting anisotropy of the doublets and the anisotropy energy K_{ac}^0 stabilizing the Γ_2 phase. It follows from the condition $K_{ac}(T_R) = 0$ and from Eq. (4) that $K_{ac}^0 = -0.432 \text{ K}$ ($\kappa = 0.3$). Since $K_{ac}^{\text{Cr}} > 0$ (Ref. 9), the negative value of K_{ac}^0 is clearly due to the large Van Vleck contribution, as in the case of DyCrO_3 (Ref. 2).

The nature of the $\Gamma_2 \rightleftharpoons \Gamma_4$ transition is governed by the sign of the coefficient in front of G_z^4 which occurs in the expression for $\Delta \Phi$ in the system (8); this term is positive but very small. Hence it follows that the $\Gamma_2 \rightleftharpoons \Gamma_4$ reorientation occurs smoothly via an intermediate canted phase Γ_{24} , but this happens in a very narrow temperature interval ($\Delta T \approx 0.2 \text{ K}$), which is manifested experimentally (Fig. 1) as an abrupt change in the spontaneous weak ferromagnetic moments m_x and m_z at $T \approx T_R$.

The $\Gamma_4(G_x) \rightleftharpoons \Gamma_1(G_y)$ transition in the ab plane, which

occurs because of the anisotropy of the exchange splitting of the Er^{3+} doublet in the phases Γ_1 and Γ_4 , is a clear first-order phase transition and it occurs when $K_{ab}(T_M) = 0$. The formal reason for this nature of the reorientation process is the relatively large positive value of the fourth-order anisotropy constant K'_{ab} , which suppresses the canted phase Γ_{14} . The physical reason is the special nature of the behavior of the splitting of the Er^{3+} doublet. Since $\Delta_y - \Delta_x \ll \Delta_{x,y}$, it follows from Eq. (3) that in the case of smooth reorientation the splitting of the doublets of the Er^{3+} ions occupying one of the inequivalent positions with

$$\varphi = \arctg(G_y/G_x) = \arctg(\Delta_x/\Delta_y) \approx 45^\circ$$

passes through zero, which is not favored by energy considerations so that an abrupt $\Phi \Pi \Gamma_4 \rightleftharpoons \Gamma_1$ phase transition takes place.

We shall first consider the field-induced orientational transitions.

H||a. Both $\Gamma_{24}(G_x G_z) \rightleftharpoons \Gamma_2(G_z)$ and $\Gamma_{12}(G_y G_z) \rightleftharpoons \Gamma_2(G_z)$ transitions occur smoothly in the relevant ac ($T > T_Q$) and bc ($T < T_Q$) planes, and their fields are given by the expressions

$$\Gamma_{24} \rightleftharpoons \Gamma_2: \left. \frac{\partial^2 \Phi}{\partial \theta^2} \right|_{\theta=0, \varphi=0} = 0, \quad \chi_{\perp} H_x^2 + m_x H_x = K_{ac}, \quad (9)$$

$$\Gamma_{12} \rightleftharpoons \Gamma_2: \left. \frac{\partial^2 \Phi}{\partial \theta^2} \right|_{\theta=0, \varphi=\pi/2} = 0, \quad m_x H_x = K_{ac} - K_{ab}, \quad (10)$$

where θ and φ are the angles governing the orientation of the vector $\mathbf{G} = (\sin \theta \cos \varphi, \sin \theta \sin \varphi, \cos \theta)$.

In the direct vicinity of the Morin point within the interval $T_M < T < T_Q$ there is a characteristic first-order transition between the phases Γ_{12} and Γ_{24} in the course of which the antiferromagnetic vector is reoriented abruptly from the bc to the ac plane. If we find the orientation of the vector \mathbf{G} for these phases

$$\begin{aligned} \Gamma_{24}: \varphi=0, \quad \cos \theta = m_x H_x / (K_{ac} - \chi_{\perp} H_x^2), \\ \Gamma_{12}: \varphi=\pi/2, \quad \cos \theta = m_x H_x / (K_{ac} - K_{ab}), \end{aligned} \quad (11)$$

and equate the corresponding thermodynamic potentials obtained for the field of the $\Gamma_{12} \rightleftharpoons \Gamma_{24}$ transition,^{10,11} we obtain

$$\chi_{\perp} H_x^2 = K_{ab}. \quad (12)$$

This a spin-flop transition (but not in a plane as is usually observed, but in space), i.e., it is due to the difference between the susceptibility of the Cr system along the a axis in the Γ_{12} and Γ_{24} phases and not due to the interaction of the weakly ferromagnetic moment m_x with the external field.

Figure 5 shows the experimental and theoretical H_x - T phase diagrams of $\text{Dy}_{1-x}\text{Er}_x\text{CrO}_3$ ($x = 0.3$). Calculations of the theoretical temperature dependences of the threshold fields were carried out using Eqs. (9), (10), and (12), but allowing for the demagnetizing field characterized by $N_x = 5$. At low temperatures and in high fields, when the approximation of Eq. (7) is no longer valid, we obtain equations of the (10) type for the field of the $\Gamma_{12} \rightleftharpoons \Gamma_2$ transition when m_x and $K_{ac} - K_{ab}$ depend on the field:

$$\begin{aligned} m_x = m_x^0 + \chi \mu_x^0 \Delta_z^0 / T_0(H_x) + (1-x) \bar{\mu}_x \Delta_z / T_1(H_x), \\ K_{ac} - K_{ab} = K_{ac}^0 - K_{ab}^0 - \chi (\Delta_z^0)^2 / T_0(H_x) \\ + (1-x) (\Delta_y^2 - \Delta_z^2) / T_1(H_x), \end{aligned} \quad (13)$$

where

$$\begin{aligned} T_0 = \Delta_{Dy} / \text{th}(\Delta_{Dy}/T), \quad T_1 = \Delta_{Er} / \text{th}(\Delta_{Er}/T), \\ \Delta_{Dy} = \mu_x^0 H_x + \Delta_z^0, \quad \Delta_{Er}^2 = \mu_x^2 H_x^2 + 2\bar{\mu}_x H_x \Delta_z + \Delta_z^2. \end{aligned}$$

At high temperatures T ($T \gg \Delta_R$) the system (13) reduces to the system (10).

It follows from the condition for the best match between the theoretical and experimental H_x - T phase diagrams and from a comparison of the calculated and experimental temperature dependences of the weakly ferromagnetic moments (Fig. 1) that the main parameters of the magnetic interactions are as follows:¹

$$\begin{aligned} \Delta_x = 4.5 \text{ K}, \quad \Delta_y = 5.5 \text{ K}, \quad \Delta_z = 2.5 \text{ K}, \\ K_{ab}^0 = 0.93 \text{ K}, \quad K_{ac}^0 = -0.67 \text{ K}, \quad m_x^0 = 0.18 \mu_B, \quad m_z^0 = 0.13 \mu_B. \end{aligned} \quad (14)$$

The values of K_{ab}^0 and K_{ac}^0 were determined in terms of Δ_i ($i = x, y, z$) using the conditions $K_{ab}(T_M) = 0$ and $K_{ac}(T_R) = 0$. The quantities $\mu_{x,zz}$ and $\bar{\mu}_x$, and the center of gravity of the splitting of the doublet $\Delta_{Er} = \frac{1}{3} \sum_i \Delta_i = 4.15$ K were taken from the published data³ [see Eq. (4b)], the susceptibility was taken to be $\chi_{\perp} = 2.5 \times 10^{-5} \text{ cm}^3/\text{g}$, and the differences $\Delta_x - \Delta_y$ and $\Delta_x - \Delta_z$ were varied. It is clear from Figs. 1 and 5 that on the whole a satisfactory description could be provided of the H_x - T diagram and of the temperature dependences $m_{m,z}(T)$. A characteristic feature of the H_x - T diagram was the bicritical point Q , where two second-order phase transition lines and a first-order phase transition line converged. Such a point had been observed earlier for $\text{DyFe}_{1-x}\text{Al}_x\text{O}_3$ (Ref. 12) and discussed in Refs. 11 and 13 for DyFeO_3 ; judging by the data of Ref. 4, it should appear also in the H_x - T phase diagram of pure ErCrO_3 .

H||c. If $T > T_R$, then in this geometry a smooth reorientation $\Gamma_{24} \rightleftharpoons \Gamma_4$ takes place in a field found from the condition

$$\left. \frac{\partial^2 \Phi}{\partial \theta^2} \right|_{\varphi=0, \theta=\pi/2} = 0, \quad \chi_{\perp} H_x^2 + m_x H_x = -K_{ac}. \quad (15)$$

At temperatures $T < T_M$ in a field **H||c** there is a first-order transition $\Gamma_{14} \rightleftharpoons \Gamma_4$. The abrupt change in the angle φ , governing the orientation \mathbf{G} in the ab plane, is shown by an analysis to be close to 90° , which is a consequence of the suppression of the canted phase Γ_{14} mentioned above. On the assumption of a 90° abrupt change in the angle φ , we can use the condition of equality of the corresponding values of the thermodynamic potential of Eq. (4) to deduce the following equation:

$$H_z = \mu_{zz}^{-1} \{ T \text{arch}[\text{ch}(\Delta_y/T) e^{-h(1+\varepsilon^2)^{1/2}}] - \Delta_x \}, \quad (16)$$

where

$$h = \frac{K_{ab}^0/2 + m_z^0 H_z}{(1-x)T}, \quad \varepsilon = \frac{\text{sh}(\mu_{zz} H_z/T)}{\text{ch}(\Delta_y/T)} \ll 1$$

At temperatures $T \lesssim T_M$ it follows from Eq. (16) that on approach to $T \rightarrow T_M$ the threshold field becomes

$$H_z^{\text{th}} \approx -K_{ab}(T)/2m_z(T) \rightarrow 0,$$

whereas in the limit $T \rightarrow 0$ we obtain (for $x = 0.3$)

$$H_z^{\text{th}} \approx [(1-x)(\Delta_y - \Delta_x) - K_{ab}^0/2] [(1-x)\mu_{zz} + m_z^0]^{-1} \approx 0.9 \text{ kOe}.$$

Figure 3 shows the temperature dependence $H_z(T)$ calculated allowing for the demagnetizing field and for the existence of a region of an intermediate state, using the parameters given above which describe well the independent experimental data obtained at low temperatures. In view of the fact that the sample was of irregular shape, the demagnetization factor N_z was deduced from the condition of the best match between the upper limit of the intermediate state $\tilde{H}_z^{\text{th}} = H_z^{\text{th}} + N_z \Delta M_z$ and the experimental result, where H_z^{th} is the threshold field found from Eq. (16) and ΔM_z is the abrupt change in the magnetization on transition to the Γ_4 phase. The discrepancy between the theory and experiment relatively high ($T > 30$ K) temperature is clearly due to the influence of the excited states of the Er^{3+} and Dy^{3+} ions on the anisotropy energy.

CONCLUSIONS

We shall now summarize the main results of the investigation. Cooling of $\text{Dy}_x\text{Er}_{1-x}\text{CrO}_3$ ($x = 0.2, 0.3$) crystals in the absence of an external magnetic field induced consecutively all three main spin configurations: $\Gamma_2(G_z)$, $\Gamma_4(G_x)$, and $\Gamma_1(G_y)$, which had not been observed before for orthochromites. An investigation was made of the various orientational transitions induced by a magnetic field $\mathbf{H} \parallel \mathbf{c}$ and the corresponding H - T phase diagrams were obtained. In particular, for $\mathbf{H} \parallel \mathbf{a}$ near the Morin point T_M we observed in addition to the usual reorientation in the ac and bc planes, also a first-order transition (of the spatial spin-flop type) between canted phases Γ_{12} and Γ_{24} . The H_x - T phase diagram had a bicritical point corresponding to convergence of two second-order phase transition lines ($\Gamma_{24} \rightleftharpoons \Gamma_2$ and $\Gamma_{12} \rightleftharpoons \Gamma_2$) and one first-order phase transition line ($\Gamma_{12} \rightleftharpoons \Gamma_{24}$).

The H_x - T and H_z - T phase diagrams found by calculation agreed with the experimental results. The parameters of the main magnetic interactions in the system were deter-

mined. It was established that the nature of the $\Gamma_1 \rightleftharpoons \Gamma_4$ abrupt Morin transition, involving a first-order phase transition (both in ErCrO_3 and $\text{Dy}_x\text{Er}_{1-x}\text{CrO}_3$), was related to a special feature of the splitting of the ground-state doublet of Er^{3+} on rotation of \mathbf{G} in the ab plane, namely its reduction to $\varphi \approx 45^\circ$ for one of the inequivalent positions of the Er^{3+} ions.

¹⁾In the calculation of $m_x(T)$ at $T \sim T_N$ we allowed (using the molecular field theory) for a reduction in the magnetic moment of the Cr^{3+} sublattices or the modulus of the antiferromagnetic vector \mathbf{G} .

¹⁾K. Tsushima *et al.*, Proc. Intern. Conf. on Magnetism, Moscow, 1973 (ed. by N. N. Sirota), Vol. 5, Nauka, Moscow (1974), p. 270.

²⁾A. M. Kadomtseva, A. K. Zvezdin, A. A. Mukhin, I. A. Zorin, I. B. Krynetskiĭ, M. D. Kuz'min, and M. M. Lukina, Zh. Eksp. Teor. Fiz. **92**, 179 (1987) [Sov. Phys. JETP **65**, 101 (1987)].

³⁾A. Hasson, R. M. Hornreich, Y. Komet, B. M. Wanklyn, and I. Yaeger, Phys. Rev. B **12**, 5051 (1975).

⁴⁾K. Toyokawa, S. Kurita, and K. Tsushima, Phys. Rev. B **19**, 274 (1979).

⁵⁾M. Eibschutz, R. L. Cohen, and K. W. West, Phys. Rev. **178**, 572 (1969).

⁶⁾H. Schuchert, S. Hufner, and R. Faulhaber, Z. Phys. B **220**, 273 (1969).

⁷⁾K. P. Belov, A. K. Zvezdin, A. M. Kadomtseva, and R. Z. Levitin, Orientational Transitions in Rare-Earth Magnetic Materials [in Russian], Nauka, Moscow (1979).

⁸⁾A. K. Zvezdin, V. M. Matveev, A. A. Mukhin, and A. I. Popov, Rare-Earth Ions in Magnetically Ordered Crystals [in Russian], Nauka, Moscow (1985).

⁹⁾I. S. Jacobs, F. Burne, and L. M. Levinson, J. Appl. Phys. **42**, 1631 (1971).

¹⁰⁾A. I. Mitsek and N. P. Kolmakova, Fiz. Met. Metalloved. **22**, 161 (1966).

¹¹⁾V. V. Eremenko, S. L. Gnatchenko, N. F. Kharchenko, P. P. Lebedev, K. Piotrowski, H. Szymczak, and R. Szymczak, Europhys. Lett. **4**, 1327 (1987).

¹²⁾V. N. Derkachenko, A. K. Zvezdin, A. M. Kadomtseva, *et al.*, Abstracts of Papers presented at All-Union Conf. on Low-Temperature Physics, Kharkov, 1980 [in Russian], Part II, Physicotechnical Institute of Low Temperatures, Academy of Sciences of the Ukrainian SSR, Kharkov (1980), p. 159.

¹³⁾P. Yu. Marchukov and E. G. Rudashevskii, Kratk. Soobshch. Fiz. No. 7, 53 (1987).

Translated by A. Tybulewicz